

# A Highly Efficient Solar Cell Made from a Dye-Modified ZnO-Covered TiO<sub>2</sub> Nanoporous Electrode

Zhong-Sheng Wang,<sup>†,‡</sup> Chun-Hui Huang,<sup>\*,†</sup> Yan-Yi Huang,<sup>†</sup> Yuan-Jun Hou,<sup>§</sup>  
Pu-Hui Xie,<sup>§</sup> Bao-Wen Zhang,<sup>§</sup> and Hu-Min Cheng<sup>||</sup>

State Key Laboratory of Rare Earth Materials Chemistry and Applications,  
Peking University–The University of Hong Kong Joint Laboratory in Rare Earth Materials  
and Bioinorganic Chemistry, Peking University, Beijing 100871, P. R. China,  
Department of Chemistry, College of Science, Shandong Agricultural University,  
Taian 271018, P. R. China, Institute of Photographic Chemistry, Chinese Academy of Science,  
Beijing 100101, P. R. China, and College of Chemistry and Molecular Engineering,  
Peking University, Beijing 100871, P. R. China

Received March 16, 2000. Revised Manuscript Received November 27, 2000

A photoelectrochemical solar cell based on porous ZnO-covered TiO<sub>2</sub> film has been fabricated with ruthenium bipyridyl complex as the sensitizer. The cell generated a short-circuit photocurrent of 21.3 mA cm<sup>-2</sup> and an open-circuit voltage of 712 mV under irradiation of 81.0 mW cm<sup>-2</sup> white light from a xenon lamp with an overall conversion efficiency of 9.8%. Compared with the pure TiO<sub>2</sub> (anatase) film, the ZnO-covered TiO<sub>2</sub> film possesses more outstanding ability to transport electrons with an overall power conversion efficiency increase by 27.3%. Optical electrochemical studies show that surface modification of TiO<sub>2</sub> with ZnO can increase the concentration of free electrons in the conduction band of TiO<sub>2</sub>. This result implies that the charge recombination is reduced in the process of electron transport through the porous network, which can decrease the photocurrent loss and hence improve both short-circuit photocurrent and open-circuit photovoltage.

## Introduction

Overall power conversion efficiency<sup>1,2</sup> reaching 10% for dye sensitized solar cell makes its practical applications feasible and, hence, brings about great attention to this field. Besides TiO<sub>2</sub>,<sup>1–3</sup> other semiconductors, such as SnO<sub>2</sub>,<sup>4</sup> Fe<sub>2</sub>O<sub>3</sub>,<sup>5</sup> ZrO<sub>2</sub>,<sup>6</sup> Al<sub>2</sub>O<sub>3</sub>,<sup>7</sup> ZnO,<sup>8</sup> et al., have also been studied for photoelectric conversion. Among all those materials studied, whether single<sup>4–8</sup> or composite<sup>9</sup> or doped<sup>10</sup> or undoped,<sup>1–8</sup> however, few other semicon-

ductors could match TiO<sub>2</sub> in solar energy conversion. On the other hand, although ZnO possesses an energy band similar to that of TiO<sub>2</sub>, *cis*-dithiocyanato[*N*-bis-(4,4'-bipyridyl-2,2'-dicarboxylic acid)]ruthenium(II) (*cis*-Ru) sensitized nanocrystalline ZnO generated a much lower yield.<sup>8</sup> In fact, nanostructured TiO<sub>2</sub> is not perfect yet in that electron transport becomes more difficult with the increase of photocurrent in the absence of space charge layer.<sup>11</sup> The efficiency of dye-sensitized nanocrystalline solar cells is limited in part by back-reaction of photoinjected electrons with triiodide ions in the electrolyte,<sup>12</sup> and the presence of electron acceptors, such as oxygen and iodine, will lead to loss of photogenerated electrons over the nanostructured semiconductor electrolyte interface during the transport of the electrons to the back contact.<sup>13</sup> The mechanism of the charge transport through the nanometer particles is not known in detail yet. However, different mechanisms for the charge transport, e.g. a hopping mechanism,<sup>14</sup> tunneling through potential barriers between the particles,<sup>15,16</sup> a trapping/detrapping mechanism,<sup>17,18</sup> and a

\* To whom correspondence should be addressed. Tel.: +86-(10)-62757156. Fax: +86-(10)62751708. E-mail: hch@chemms.chem.pku.edu.cn.

<sup>†</sup> State Key Laboratory of Rare Earth Materials Chemistry and Applications, Peking University.

<sup>‡</sup> Shandong Agricultural University.

<sup>§</sup> Chinese Academy of Science.

<sup>||</sup> College of Chemistry and Molecular Engineering, Peking University.

- (1) O'Regan, B.; Grätzel, M. *Nature (London)* **1991**, *353*, 737.
- (2) Nazeeruddin, M. K.; Kay, A.; Rodicio, I.; Humphry-Baker, R.; Müller, E.; Liska, P.; Vlachopoulos, N.; Grätzel, M. *J. Am. Chem. Soc.* **1993**, *115*, 6382.
- (3) O'Regan, B.; Moser, J.; Anderson, M.; Grätzel, M. *J. Phys. Chem.* **1990**, *94*, 8720.
- (4) Dabestani, R.; Bard, A. J.; Campion, A.; Fox, M. A.; Mallouk, T. E.; Webber, S. E.; White, J. M. *J. Phys. Chem.* **1988**, *92*, 1872.
- (5) Fitzmaurice, D. J.; Frei, H. *Langmuir* **1991**, *7*, 1129.
- (6) Heimer, T. A.; D'Arcangelis, S. T.; Farzad, F.; Stipkala, J. M.; Meyer, G. J. *Inorg. Chem.* **1996**, *35*, 5319.
- (7) Nüesch, F.; Moser, J. E.; Shklover, V.; Grätzel, M. *J. Am. Chem. Soc.* **1996**, *118*, 5420.
- (8) Rensmo, H.; Keis, K.; Lindström, H.; Södergren, S.; Solbrand, A.; Hagfeldt, A.; Lindquist, S.-E.; Wang, L. N.; Muhammed, M. *J. Phys. Chem. B* **1997**, *101*, 2598.
- (9) (a) Tennakone, K.; Kumara, G. R. R. A.; Kottegoda, I. R. M.; Perera, V. P. S. *Chem. Commun.* **1999**, 15. (b) Tennakone, K.; Kottegoda, I. R. M.; De Silva L. A. A.; Perera, V. P. S. *Semicond. Sci. Technol.* **1999**, *14*, 975.

(10) Wang, Y. Q.; Cheng, H.-M.; Hao, Y.-Z.; Ma, J.-M.; Li, W.-H.; Cai, S.-M. *J. Mater. Sci.* **1999**, *34*, 3721.

(11) Hagfeldt, A.; Grätzel, M. *Chem. Rev.* **1995**, *95*, 49.

(12) Peter, L. M.; Wijayantha, K. G. U. *Electrochem. Commun.* **1999**, *1*, 576.

(13) Rensmo, H.; Lindstrom, H.; Sodergren, S.; Willstedt, A.-K.; Solbrand, A.; Hagfeldt, A.; Lindquist, S.-E. *J. Electrochem. Soc.* **1996**, *143*, 3173.

(14) Könenkamp, R.; Henninger, R.; Hoyer, P. *J. Phys. Chem.* **1993**, *97*, 7328.

(15) Hoyer, P.; Eichberger, R.; Weller, H. *Ber. Bunsen-Ges. Phys. Chem.* **1993**, *97*, 636.

(16) Hoyer, P.; Weller, H. *J. Phys. Chem.* **1995**, *99*, 14096.

diffusion model,<sup>12,17,19</sup> have been proposed, and the properties of electron transport through nanostructured TiO<sub>2</sub> particles have been studied by several authors.<sup>16,17,19–21</sup> No matter which mechanism is reasonable, the charge transport in the cis-Ru-coated TiO<sub>2</sub> film is no doubt a key step for further increasing the short-circuit photocurrent ( $I_{sc}$ ) and consequently the overall power conversion yield ( $\eta$ ).

A rather unusual feature of these nanocrystalline films is lack of a depletion layer at the nanostructured semiconductor/electrolyte interface.<sup>3,11,22–24</sup> As a result, the back electron transfer, i.e., the charge recombination between the electrons injected in the conduction band (CB) of the semiconductor and the oxidized sensitizer, still remains one of the major limiting factors to the efficiency of the dye sensitized solar cells. If one can improve TiO<sub>2</sub> film to further reduce the charge recombination, the overall power conversion efficiency would be increased. Cheng et al. reported that the doping of Zn<sup>2+</sup> ion into TiO<sub>2</sub> at pH 1.8 could increase the quantum efficiency for photoelectric conversion under ultraviolet light excitation, especially at about 320 nm.<sup>10</sup> Could Zn<sup>2+</sup> ion improve the property of electron transport in more extended wavelength range? To explore this question, we tried to modify the TiO<sub>2</sub> surface with ZnO, and this method has been proved to improve the performance of the Grätzel cell remarkably.

### Experimental Section

**Materials.** Optically transparent conducting glass (CTO glass, fluorine-doped SnO<sub>2</sub> overlayer, transmission > 70% in the visible, sheet resistance 20  $\Omega$ /square) was obtained from the Institute of Nonferrous Metals of China. Titanium tetraisopropoxide, 4-*tert*-butylpyridine, propylene carbonate (PC), and ethylene carbonate (EC) were purchased from Acros. All the other solvents and chemicals used in the experiments are at least reagent grade (Beijing Chemical Factory, Beijing, China) and used without further purification. Tetrabutylammonium perchlorate (TBAP), lithium perchlorate, and acetonitrile (MeCN) were dried according to the method described in the literature.<sup>25,26</sup> The redox electrolyte used in this work is always 0.3 M LiI + 0.03 M I<sub>2</sub> in a PC/EC (1:1, v/v) mixture solvent. cis-Ru was synthesized according to the literature,<sup>2</sup> and its purity was confirmed by <sup>1</sup>H NMR and elemental analysis.

**Preparation of Colloids.** A 100–150 g dm<sup>-3</sup> TiO<sub>2</sub> colloidal dispersion, containing 40 wt % poly(ethylene glycol) (MW 20 000), was prepared by following the procedure reported in the literature,<sup>1</sup> except that autoclaving was performed at 220 °C instead of 200 °C. ZnO-covered TiO<sub>2</sub> (TiO<sub>2</sub>-Zn) colloid was prepared via the hydrothermal method. After addition of 18.8 mg of ZnCl<sub>2</sub> to 15 cm<sup>3</sup> of 2 M TiCl<sub>4</sub> aqueous solution, the mixture was adjusted to pH 5 with KOH solution under vigorous stirring. The mixture was autoclaved at 170 °C for 3

h under continuous stirring and then allowed to cool overnight. The yielded precipitate was filtered out and washed with HAc–NH<sub>4</sub>Ac (pH 5) and C<sub>2</sub>H<sub>5</sub>OH successively, which could prevent the peptization of the precipitate. Part of the precipitate was dried at 120 °C and subsequently heated at 450 °C for 30 min. The white powder product was used to perform XRD analysis. Adequate water was added to the remaining precipitate to form a 100–150 g dm<sup>-3</sup> suspension, which was peptized with 68% nitric acid (about 0.1 cm<sup>3</sup>) and dispersed ultrasonically for 30 min to form stable colloid. To prevent cracking during film drying, poly(ethylene glycol) (MW 20 000) was added to TiO<sub>2</sub>-Zn colloid in a proportion of 80% of the TiO<sub>2</sub> weight. Additionally, 2 wt % Triton X-100 was added to both TiO<sub>2</sub> and TiO<sub>2</sub>-Zn colloids to facilitate their spreading on CTO glass.

**Preparation of Electrodes.** To improve the ohmic contact between TiO<sub>2</sub> particles and CTO glass, 3 drops of 1  $\times$  10<sup>-3</sup> M titanium tetraisopropoxide in 2-propanol was spread on the conducting glass (2  $\times$  8 cm) and dried naturally in air at room temperature. Then 3 drops of the colloid was spread uniformly onto the top of the first layer followed by annealing at 450 °C in air flow for 30 min. The 8- $\mu$ m-thick TiO<sub>2</sub> and TiO<sub>2</sub>-Zn films were obtained after repeating the above procedure several times. Before being immersed in the dye solution, these films were soaked in the 0.2 M aqueous TiCl<sub>4</sub> solution overnight followed by washing with deionized water and heating again at 450 °C.

Coloration of the TiO<sub>2</sub> surface with the dye was carried out by immersing the film (still warm, i.e., 80–100 °C) for at least 12 h in a 3  $\times$  10<sup>-4</sup> M solution of cis-Ru in absolute ethanol.<sup>2</sup> Before wetted with redox electrolyte solution for testing, the dye-coated film was soaked in 4-*tert*-butylpyridine for 30 min to improve the open-circuit photovoltage ( $V_{oc}$ ).<sup>2</sup> The roughness factors, defined as the ratio of total surface area to geometric area of the film, are derived to be 870 for TiO<sub>2</sub>-Zn (abs = 1.25) and 1100 for TiO<sub>2</sub> (abs = 1.56) films according to the method reported in the literature.<sup>2</sup>

**Methods.** The thickness of the film was determined with a DEKTAK 3 profilometer. Absorption spectra were recorded with a Shimadzu UV-3100 spectrophotometer. X-ray diffraction (XRD) was carried out in Rigaku Dmax-2000 diffractometer using Cu K $\alpha$  radiation at 40 kV, 100 mA with a graphite monochromator. The colloidal particle sizes and their electron diffraction patterns were determined by JEM-200CX transmission electron microscope (TEM) at 100 kV. The current–voltage characteristic curves were recorded in a standard 2-electrode system described elsewhere.<sup>27</sup> 4-*tert*-butylpyridine treated dye-coated film was used as working electrode, the effective area for illumination being 0.30 cm<sup>2</sup>. The counter electrode was ITO glass on which 200-nm-thick layer of Pt was deposited by sputtering. A 500 W xenon lamp (Ushio Electric, Tokyo, Japan) was used as a light source. Light intensities were measured with a Light Gauge Radiometer/Photometer (Coherent, Auburn, CA) which was newly checked before used. The output light intensity from xenon lamp was measured after the UV-cutoff filter and the IR filter had been put into the beam. The effect of bias voltage on dark current for dye-coated film was measured with a model 600 voltammeteric analyzer (CH Instruments Inc., Cordova, TN). A three-electrode cell was comprised of a dye-coated film working electrode, a platinum wire as counter electrode, and a saturated calomel electrode (SCE) as reference electrode. Before measurement, the redox electrolyte was degassed with ultrapure nitrogen for 15 min. For spectroscopic electrochemistry measurement, 8- $\mu$ m-thick TiO<sub>2</sub> or TiO<sub>2</sub>-Zn film formed the working electrode (3.0 cm<sup>2</sup> surface area) of a three-electrode single compartment cell, the counter electrode being platinum wire and the reference electrode a Ag/AgCl electrode. The electrolyte solution was 0.2 M TBAP in MeCN containing 0.1 M LiClO<sub>4</sub>. Potential control was carried out on a model 600 voltammeteric analyzer, while a Shimadzu UV-3100 spectrophotometer was used to record the absorbance changes at 780

(17) De Jongh, P. E.; Vanmaekelbergh, D. *J. Phys. Chem. B* **1997**, *101*, 2716.

(18) Schwarzburg, K.; Willig, F. *Appl. Phys. Lett.* **1991**, *58*, 2520.

(19) Sodergren, S.; Hagfeldt, A.; Olsson, J.; Lindquist, S.-E. *J. Phys. Chem.* **1994**, *98*, 5552.

(20) Vanmaekelbergh, D.; De Jongh, P. E. *J. Phys. Chem. B* **1999**, *103*, 747.

(21) Solbrand, A.; Henningsson, A.; Sodergren, S.; Lindstrom, H.; Hagfeldt, A.; Lindquist, S.-E. *J. Phys. Chem. B* **1999**, *103*, 1078.

(22) Curran, J. S.; Lamouche, D. *J. Phys. Chem.* **1983**, *87*, 5405.

(23) Hagfeldt, A.; Bjorksten, U.; Lindquist, S. E. *Sol. Energy Mater. Sol. Cells* **1992**, *27*, 293.

(24) Albery, W.; Bartlett, P. N. *J. Electrochem. Soc.* **1984**, *131*, 315.

(25) Redmond, G.; Fitamaurice, D. *J. Phys. Chem.* **1993**, *97*, 1426.

(26) Rothenberger, G.; Fitzmaurice, D.; Grätzel, M. *J. Phys. Chem.* **1992**, *96*, 5983.

(27) Smestad, G. P.; Grätzel, M. *J. Chem. Educ.* **1998**, *75*, 752.

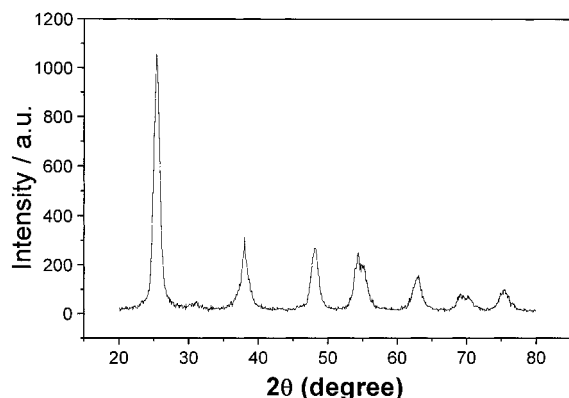


**Figure 1.** XRD pattern of the  $\text{TiO}_2$ -Zn powder product, which is coincide with the standard one for anatase.

nm for the determination of the flat band potential of the nanostructured film.

### Results and Discussion

**Characterization of ZnO-Covered  $\text{TiO}_2$  Nanoparticles.** The result of ICP analysis shows that 0.46 mol % ZnO of  $\text{TiO}_2$  was found in  $\text{TiO}_2$ -Zn powder, which is coincide with its initial addition amount 0.5 mol %. In fact,  $\text{Zn}^{2+}$  can be hydrolyzed completely at pH 5, so it was hardly lost during the preparation of colloid. To clarify the effect of ZnO covering on the morphology and size of  $\text{TiO}_2$  particles. A TEM and electron diffraction study was performed, the results showing that ZnO-covered and uncovered  $\text{TiO}_2$  colloidal particles are both in the polycrystalline state and about 10 nm in diameter. This result implies that the covering of ZnO has little effect on the formation of  $\text{TiO}_2$  particles. Furthermore,  $\text{TiO}_2$ -Zn powder was still in pure anatase phase supported by its XRD result (Figure 1), in which no separate ZnO phase or other phase was detected. Therefore, we can exclude the possibility of  $\text{Zn}^{2+}$  substituting the lattice position of  $\text{Ti}^{4+}$ ; otherwise the XRD peaks for anatase would be shifted to some extent. It can be inferred from the results of XRD and ICP that  $\text{Zn}^{2+}$  ion should be adsorbed onto the surface of  $\text{TiO}_2$  particles. This conclusion is also supported by another fact that the initial pH of precipitation<sup>28</sup> is 0.5 for  $\text{Ti}^{4+}$  and 6.7 for  $\text{Zn}^{2+}$ .  $\text{Ti}^{4+}$  ion will precipitate first and then be followed by the precipitation of  $\text{Zn}^{2+}$  with gradually increasing pH of the mixture. Therefore, one can conclude that  $\text{Zn}^{2+}$  ion is adsorbed onto the  $\text{TiO}_2$  surface and turns into ZnO after annealing.

**Current-Voltage Characteristics.** To avoid the excitation of ultraviolet light on  $\text{TiO}_2$ -Zn or  $\text{TiO}_2$  semiconductor, a GG420 filter was used to cut off the light with wavelength less than 420 nm. Under irradiation of white light from a xenon lamp with a GG420 filter and an IRA-25S filter in the light beam to cut off the light less than 420 nm and infrared light, no photocurrents were detected for both bare  $\text{TiO}_2$ -Zn and  $\text{TiO}_2$  films. Under irradiation of 81.0  $\text{mW cm}^{-2}$  white light from a Xe lamp ( $\lambda > 420$  nm), the cell gave a short-circuit photocurrent ( $I_{sc}$ ) of 21.3  $\text{mA cm}^{-2}$ , open-circuit photovoltage ( $V_{oc}$ ) of 712 mV, and fill factor (FF) of 0.52, corresponding to 9.8% of overall yield ( $\eta$ ), as shown in

**Table 1.** Comparison of the Performance Parameters of the Cells Based on  $\text{TiO}_2$ -Zn Films and  $\text{TiO}_2$  Films

	$\text{TiO}_2$ -Zn film					$\text{TiO}_2$ film	
	13.6	52.2	68.2	81	101.9	81 <sup>b</sup>	96 <sup>c</sup>
$P_{in}$ / $\text{mW cm}^{-2}$	4.93	15.4	18.5	21.3	25.3	18.2	18.2
$I_{sc}$ / $\text{mA cm}^{-2}$	684	710	744	712	712	663	720
$V_{oc}$ /mV	0.70	0.57	0.57	0.52	0.50	0.52	0.73
FF (%)	17.4	12.0	11.5	9.8	8.9	7.7	10.0

<sup>a</sup> Absorbance of dye-coated  $\text{TiO}_2$ -Zn film was 1.25. A GG420-cutoff filter was used to cut off light below 420 nm, and an IRA-25S filter was used to cut off infrared light. <sup>b</sup> Absorbance of dye-coated  $\text{TiO}_2$  film was 1.56. The cell was based on pure  $\text{TiO}_2$  in this work; the experimental conditions are the same as those of the  $\text{TiO}_2$ -Zn electrode. <sup>c</sup> Grätzel's cell based on  $\text{TiO}_2$  cited from ref 2.

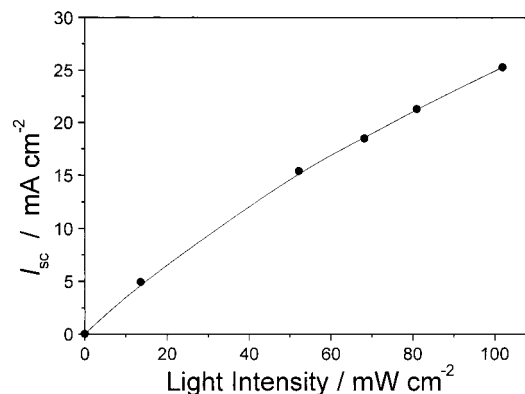


**Figure 2.** Relationship between the short-circuit photocurrents of the cell on the basis of the  $\text{TiO}_2$ -Zn and light intensities. GG420 and an IRA-25S filters were used to cut off light with wavelength less than 420 nm and greater than 800 nm, respectively.

Table 1. The fill factor (FF) is defined as

$$\text{FF} = V_{opt} I_{opt} / V_{oc} I_{sc} \quad (1)$$

where  $V_{opt}$  and  $I_{opt}$  are respectively voltage and current for maximum power output.  $\eta$  is defined in the following equation:

$$\eta = \frac{I_{sc} V_{oc} \text{FF}}{P_{in}} \quad (2)$$

Here  $P_{in}$  is the power of incident white light from a Xe lamp. Also listed in Table 1 are cell ( $\text{TiO}_2$ -Zn and  $\text{TiO}_2$ ) performance parameters at different light intensities and those for the Grätzel cell<sup>2</sup> based on  $\text{TiO}_2$  (anatase). The relationship between short-circuit photocurrent and light intensity is illustrated in Figure 2, from which we can see that short-circuit photocurrents increase with increasing light intensity in the range of 0 to 100  $\text{mW cm}^{-2}$ . The change of derivatives of the curve indicates that the photocurrent is limited by diffusion of the iodide or triiodide ions<sup>2</sup> within the nanostructured film in the current density range of 0–25  $\text{mA cm}^{-2}$ . We cannot compare the present results with those<sup>2</sup> of the Grätzel cell, since the light from a Xe lamp has more photons in the blue end of spectrum than solar light. But it is evidently seen from Table 1 that the data obtained from  $\text{TiO}_2$ -Zn electrode are much better than those from pure  $\text{TiO}_2$  electrode, since they were obtained under the same conditions.  $I$ - $V$  curves for the cell based on  $\text{TiO}_2$ -Zn and  $\text{TiO}_2$  are illustrated in Figure 3.

(28) Svehla, G. *Vogel's Textbook of Macro and Semimicro Qualitative Inorganic Analysis*, 5th ed.; Longman: London, New York, 1979.

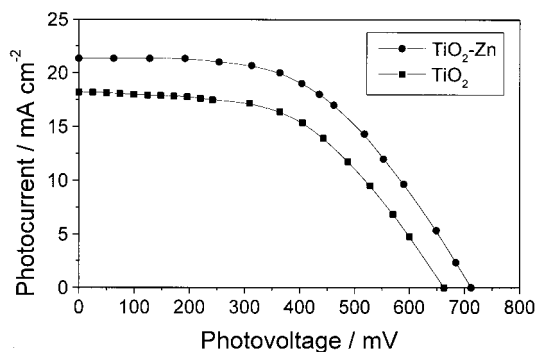


**Figure 3.**  $I$ - $V$  curves under irradiation of  $81.0 \text{ mW cm}^{-2}$  white light from Xe lamp ( $420 \text{ nm} < \lambda < 800 \text{ nm}$ ) for both dye-coated  $\text{TiO}_2$ -Zn film and dye-coated pure  $\text{TiO}_2$  film pretreated with 4-*tert*-butylpyridine.

To check the cell performance, the cells were measured under direct sunlight on May 28 in Beijing at 11:30–13:00 (light intensity is  $80.5 \text{ mW cm}^{-2}$ ). Short-circuit photocurrents were  $21.1$  and  $17.8 \text{ mA cm}^{-2}$  for  $\text{TiO}_2$ -Zn and  $\text{TiO}_2$ , respectively. We also measured the cell performance in diffuse daylight ( $10.0 \text{ mW cm}^{-2}$ ). Short-circuit photocurrents were  $2.6$  and  $2.2 \text{ mA cm}^{-2}$  for  $\text{TiO}_2$ -Zn and  $\text{TiO}_2$ , respectively. These results show that the spectral mismatch between sunlight and the Xe lamp we used is small at high intensity but large at low intensity. As comparisons under the same conditions, one can see from the photoelectrochemical results that the covering of ZnO can improve the performance of the solar cell remarkably under irradiation of  $81.0 \text{ mW cm}^{-2}$  from a Xe lamp;  $I_{sc}$  increased by  $17.0\%$  from  $18.2$  to  $21.3 \text{ mA cm}^{-2}$ ,  $V_{oc}$  increased by  $7.4\%$  from  $663$  to  $712 \text{ mV}$ ,  $\eta$  increased by  $27.3\%$  from  $7.7\%$  to  $9.8\%$ , and FF remains constant.

The stability of the dye-sensitized solar cell based on  $\text{TiO}_2$ -Zn electrode was also investigated with 4 independent samples. The stability measurements were performed every other day for 2 months, each measurement sustaining 1 h, after which short-circuit photocurrents remained almost constant for each sample. This indicates that the surface modification of  $\text{TiO}_2$  by zinc did not weaken the excellent stability of this star dye.

**Role of ZnO on  $\text{TiO}_2$ .** That no photocurrent was detected for bare  $\text{TiO}_2$ -Zn film combined with the better improvement of the cell performance after the covering of ZnO indicates that ZnO plays an important role in electron transport. Another fact that also gives a strong support to the conclusion is that the decrease of roughness factor after ZnO covering should lead to the decrease in  $I_{sc}$ , but  $I_{sc}$  increases remarkably. This phenomenon implies that  $\text{TiO}_2$ -Zn films are so favorable in electron transport that the loss of photocurrent due to the lower amount of dye adsorbed on  $\text{TiO}_2$ -Zn film can be compensated sufficiently.

(1) *Covering of ZnO Favors the Electron Transport.* Using the spectroscopic technique developed by Fitzmaurice and Grätzel,<sup>25,26</sup> the flatband potential  $V_{fb}$  of ZnO covered or uncovered nanostructured  $\text{TiO}_2$  film was determined. Absorbances at  $780 \text{ nm}$ , plotted as a function of applied potential between  $+1.00$  and  $-1.50 \text{ V}$  (vs Ag/AgCl), remain unchanged between  $+1.00$  and  $-0.98 \text{ V}$  for  $\text{TiO}_2$  and between  $+1.00$  and  $-0.86 \text{ V}$  for  $\text{TiO}_2$ -Zn, respectively, and both rise steeply at more

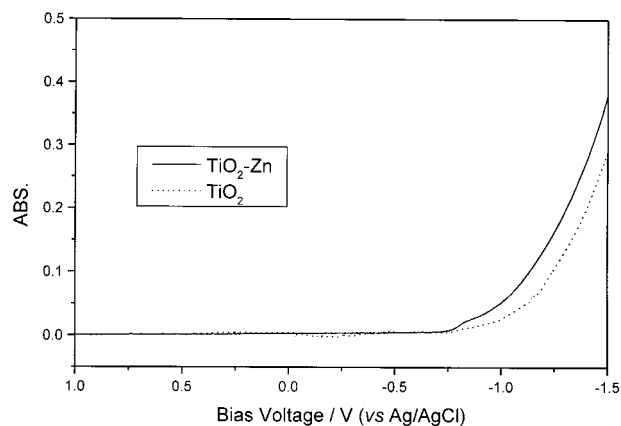


**Figure 4.** Absorbance measured at  $780 \text{ nm}$  as a function of applied potential for ZnO covered and pure  $\text{TiO}_2$  electrode in MeCN containing  $0.2 \text{ M TBAP}$  and  $0.1 \text{ M LiClO}_4$ . The scan rate was  $5 \text{ mV s}^{-1}$ .

negative potentials; see Figure 4. Therefore,  $V_{fb}$  is positively shifted by  $0.12 \text{ V}$  when ZnO covers the surface of  $\text{TiO}_2$  particles. Obviously, the energy level for electron injection is decreased after ZnO covering on the surface of  $\text{TiO}_2$  particle, which increases the driving force for electron injection and hence reduces recombination between electron injected and electron acceptors such as dye cation or triiodide ions. On the other hand, since absorbance is proportional to the concentration of free electrons<sup>25,26</sup> in the CB of semiconductor, one can see from Figure 4 that the concentration of free electrons in the CB is increased after ZnO covering the  $\text{TiO}_2$  surface at the potential range of  $-1.00$  to  $-1.50 \text{ V}$ . The above result suggests that charge recombination should be reduced upon the surface modification of  $\text{TiO}_2$  with ZnO. This implies that the number of deep trap states existing in the surface of  $\text{TiO}_2$  is decreased, and therefore, electrons transport faster after ZnO covering.<sup>17</sup> Regarding the cis-Ru-coated electrode, it is rational that the  $\text{TiO}_2$ -Zn electrode generates higher photocurrent than  $\text{TiO}_2$  does due to the reduction of charge recombination.

(2) *Covering of ZnO Suppresses the Dark Current Generation.* On the basis of energetics only, positive shift of the flat band potential should lead to decrease but not increase of the open-circuit photovoltage, which suggests that interfacial kinetics of recombination reactions should be a limiting factor for the improvement. For regenerative photoelectrochemical system, the following equation holds:<sup>29,30</sup>

$$V_{oc} = \left( \frac{kT}{e} \right) \ln \left( \frac{I_{inj}}{n_{cb} k_{et} [I_3^-]} \right) \quad (3)$$

Here  $I_{inj}$  is the flux of charge resulted from dye sensitized electron injection,  $n_{cb}$  is the concentration of electrons at the surface of  $\text{TiO}_2$ , and  $k_{et}$  is the rate constant for triiodide reduction. To investigate how ZnO covering affects recombination reactions, the effect of applied potential on the onset of dark current was studied, as shown in Figure 5. The dark current results from the reduction of triiodide by the conduction band

(29) Rosenblut, M. L.; Lewis, N. S. *J. Phys. Chem.* **1989**, *93*, 3735.

(30) Kumer, A.; Santangelo, P. G.; Lewis, N. S. *J. Phys. Chem.* **1992**, *96*, 835.

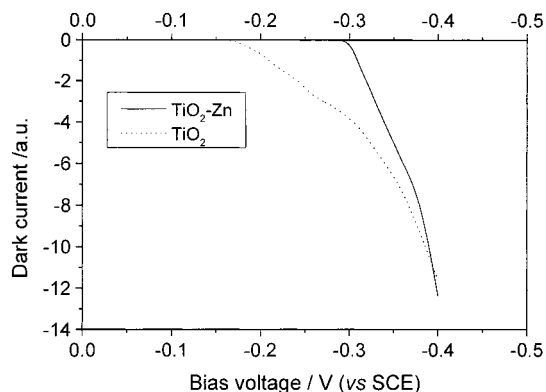


**Figure 5.** Dark current–bias voltage curves for dye-coated films pretreated with 4-*tert*-butylpyridine. A negative value for dark current stands for cathodic current.

electrons



which occurs at the surface of  $\text{TiO}_2$  particles. The triiodide either crosses the dye layer or enters into very small pores where *cis*-Ru cannot penetrate. The onset of dark current is shifted by ca.  $-130$  mV from  $-160$  to  $-290$  mV (vs SCE) after ZnO covering. This indicates that the rate constant for triiodide reduction is decreased by the covering of  $\text{TiO}_2$  with ZnO, which thus leads to the increase in the open-circuit voltage according to eq 3. Surface states, presumably represented by Ti (IV) ions, are active as intermediates in the heterogeneous charge transfer.<sup>2,31</sup> Part of the  $\text{TiO}_2$  surface is covered by ZnO, which blocks surface states and hence reduces the rate constant for the reduction of triiodide. The increase in electron concentration in the CB (Figure

4) supports the blockade of surface states. Consequently, the suppression of recombination reactions can reduce the photocurrent loss and hence improve short-circuit photocurrent. It has been confirmed that both charge separation and charge transfer occur at the surface of colloidal particles,<sup>32,33</sup> so it is not surprising that ZnO adsorbed on the  $\text{TiO}_2$  surface largely promotes the charge transport.

### Conclusions

The covering of ZnO on  $\text{TiO}_2$  better improves the property of electron transport for colloidal  $\text{TiO}_2$  film, resulting in a significant increase in short-circuit photocurrent, open-circuit photovoltage, and overall power conversion efficiency. ZnO covering leads to a positive shift of flat band potential and an increase in free electron concentration in the CB with respect to pure  $\text{TiO}_2$  film. The increase in free electron concentration after ZnO covering may be resulted from the blockade of surface states; the latter favors the charge transport and prevents loss of photogenerated electrons due to the presence of electron acceptors. As a consequence, electrons injected to the CB of  $\text{TiO}_2$ -Zn will transport to the back contact quickly. That the onset of dark current is negatively shifted by 130 mV reveals that the covering of ZnO suppresses the dark current generation and, thus, improves both open-circuit photovoltage and short-circuit photocurrent. The overall power conversion yield is, therefore, increased remarkably. The detailed mechanism study is in progress.

**Acknowledgment.** The State Key Program of Fundamental Research (G 1998061310), the NNSFC (2002-3005, 59872001, 29733100, and 29971031), and Doctoral Program Foundation of Higher Education (99000132) are gratefully acknowledged for financial support.

CM000230C

(32) Tachibana, Y.; Moser, J. E.; Grätzel, M.; Klug, D. R.; Durrant, J. R. *J. Phys. Chem.* **1996**, *100*, 20056.

(33) Ghosh, H. N.; Asbury, J. B.; Weng, Y.; Lian, T. *J. Phys. Chem. B* **1998**, *102*, 10208.

(31) Moser, J.; Punchedewa, S.; Infelta, P. P.; Grätzel, M. *Langmuir* **1991**, *7*, 3012.